A&A 481, 161–168 (2008)
DOI: 10.1051/0004-6361:20079114

Astronomy & Astrophysics

Chemical analysis of carbon stars in the Local Group⋆

II. The Carina dwarf spheroidal galaxy

C. Abia[1], P. de Laverny[2], and R. Wahlin[3]

[1] Dpto. Física Teórica y del Cosmos, Universidad de Granada, 18 071 Granada, Spain
e-mail: cabia@ugr.es
[2] Observatoire de la Côte d'Azur, Dpt. Cassiopée UMR6 202, 06 304 Nice Cedex 4, France
[3] Department of Astronomy and Space Physics, Box 515, 75120 Uppsala, Sweden

Received 21 November 2007 / Accepted 8 January 2008

ABSTRACT

Aims. We present new results of our ongoing chemical study of carbon stars in Local Group galaxies to test the critical dependence of *s*-process nucleosynthesis on the stellar metallicity.
Methods. We collected optical spectra with the VLT/UVES instrument of two carbon stars found in the Carina Dwarf Spheroidal (dSph) galaxy, namely ALW-C6 and ALW-C7. We performed a full chemical analysis using the new generation of hydrostatic, spherically symmetric carbon-rich model atmospheres and the spectral synthesis method in LTE.
Results. The luminosities, atmosphere parameters and chemical composition of ALW-C6 and ALW-C7 are compatible with these stars being in the TP-AGB phase undergoing third dredge-up episodes, although their extrinsic nature (external pollution in a binary stellar system) cannot be definitively excluded. Our chemical analysis shows that the metallicity of both stars agree with the average metallicity ([Fe/H] ~ -1.8 dex) previously derived for this satellite galaxy from the analysis of both low resolution spectra of RGB stars and the observed colour magnitude diagrams. ALW-C6 and ALW-C7 present strong *s*-element enhancements, [*s*/Fe] $= +1.6, +1.5$, respectively. These enhancements and the derived *s*-process indexes [*ls*/Fe], [*hs*/Fe] and [*hs*/*ls*] are compatible with theoretical *s*-process nucleosynthesis predictions in low mass AGB stars ($\sim$1.5 $M_{\odot}$) on the basis that the $^{13}C(\alpha, n)^{16}O$ is the main source of neutrons. Furthermore, the analysis of C_2 and CN bands reveals a large carbon enhancement (C/O $\sim$ 7 and 5, respectively), much larger than the values typically found in galactic AGB carbon stars (C/O $\sim$ 1–2). This is also in agreement with the theoretical prediction that AGB carbon stars are formed more easily through third dredge-up episodes as the initial stellar metallicity drops. However, theoretical low-mass AGB models apparently fail to simultaneously fit the observed *s*-element and carbon enhancements. On the other hand, Zr is found to be less enhanced in ALW-C7 compared to the other elements belonging to the same *s*-peak. Although the abundance errors are large, the fact that in this star the abundance of Ti (which has a similar condensation temperature to Zr) seems also to be lower than those of others metals, may indicate the existence of some depletion into dust-grains in its photosphere.

Key words. stars: abundances – stars: carbon – galaxies: dwarf – stars: AGB and post-AGB – galaxies: Local Group

1. Introduction

Due to their peculiar star formation histories, which translate into complex stellar metallicity distributions, the satellite galaxies of the Milky Way offer a unique possibility to observe intrinsic metal poor AGB stars: i.e., AGB stars that owe their chemical peculiarities to in situ nucleosynthesis and mixing processes. Furthermore, because the distances of these stellar systems are relatively well known, it is possible to derive more accurate stellar luminosities, a critical parameter for theoretical comparisons.

In this sense, the dwarf spheroidal (dSph) satellite galaxy Carina is particularly interesting among the dSphs in the Local Group because of its unusual, episodic star formation history. First indications that Carina was not purely an old globular cluster came from the discovery of several carbon stars by Cannon et al. (1981) and Mould et al. (1982). More recently, Smecker-Hane et al. (1996) by studying its colour–magnitude diagram (CMD) with deep photometry, found three well-defined, distinct main sequence turn-offs corresponding to ages of about 2, 3–6 and 11–13 Gyr, respectively. Interestingly, they note that the three main sequences connect with a unique, narrow red giant branch and conclude that regardless of the age, Carina stars are metal-poor with mean metallicity [Fe/H] $= -1.86 \pm 0.20$. Monelli et al. (2003), Rizzi et al. (2003) and Koch et al. (2006) reach the same conclusion. However, these last authors, from low resolution spectra of 437 Carina giant stars around the Ca II infrared triplet, found a much broader spread in the metallicity distribution around the above value ($FWHM \sim 0.92$), while the full range of metallicities is found to span $-3.0 \leq$ [Fe/H] ≤ 0.0. Indeed, the age-metallicity degeneracy in Carina dSph seems to form a narrow red giant branch despite the considerable spread in metallicity and age. In fact, the metallicity distribution found by Koch et al. (2006) cannot be explained by a simple closed-box model of chemical evolution. More sophisticated models, characterised by more than one episode of star formation and intense galactic winds (Lanfranchi et al. 2006), are required to explain the observed metallicity distribution in this satellite galaxy.

AGB stars are believed to be the main producers of *s*-elements in the Universe, at least for the nuclei belonging to the main and strong *s*-components ($A > 88$). There

⋆ Based on observations collected with the VLT/UT2 telescope (Paranal Observatory, ESO, Chile) using the UVES (program ID 74.D-0539) instrument.

is accumulating observational evidence that indicates that the $^{13}C(\alpha,n)^{16}O$ reaction, acting in low mass AGB stars ($M < 3\ M_{\odot}$), is the main neutron source in the *s*-process. It only requires $\sim 10^8$ K to be activated, a temperature usually attained at the top layer of the He-rich inter-shell during the interpulse periods (Gallino et al. 1998; Goriely & Siess 2001; Herwig 2005). However, the physical mechanism able to produce enough ^{13}C in the He inter-shell is not yet known (see Goriely & Siess 2004; Siess et al. 2004; Busso et al. 2006), so that it is usually assumed that a small amount of hydrogen is injected from the convective envelope into the inter-shell region at the time of the third dredge-up (TDU). At hydrogen-shell reignition, due to proton captures on ^{12}C, a ^{13}C-*pocket* forms within the inter-shell (Straniero et al. 1995). The ^{13}C produced in this way is fully consumed by α-captures during the interpulse phase, thus allowing a neutron exposure suitable for a substantial *s*-process. Then, the freshly synthesised *s*-elements are engulfed by the convective shell generated by the next thermal pulse (TP). Nevertheless, theoretical models (e.g. Busso et al. 1999; Gallino et al. 2006) show that the *s*-process is far from being a unique process. For a given initial mass and depending on the efficiency of the ^{13}C-pocket, decreasing the metallicity starting from a solar composition, the *s*-process fluency progressively feeds the first *s*-peak elements Sr, Y, Zr (light-*s*, or *ls*) then the second *s*-peak at Ba, La, Ce, Pr, Nd, Sm (heavy-*s*, or *hs*) and eventually the third *s*-peak at the termination point of the *s*-process (Pb). The *s*-element abundance patterns found in the galactic extrinsic (externally polluted) and intrinsic (internally polluted) O- and C-rich stars in a wide range of metallicity agree with this prediction (Busso et al. 2001; Aoki et al. 2002; Abia et al. 2002; Van Eck et al. 2003; Van Winckel 2003; Beers & Christlieb 2005). However, despite this broad agreement between theory and observations, the *s*-element abundance patterns also show that a wide spread in the efficiency of the ^{13}C-pocket must exist: around one or two orders of magnitude with respect to the standard (ST) case, which corresponds to the amount of ^{13}C needed for a 1.5 $M_{\odot}$ AGB star with half solar metallicity to produce the main *s*-process element abundances in the Sun (see Gallino et al. 1998, for details).

The present study is an extension of the work of de Laverny et al. (2006) (Paper I, hereafter), where one AGB carbon star in the Small Magellanic Cloud (SMC) (BMB-B 30, with metallicity [M/H] = −1.0[1]) and two in the Sagittarius dwarf Spheroidal galaxy (Sag dSph) (IGI95-C1 and IGI95-C3 with [M/H] = −0.8 and −0.5, respectively) were chemically analysed. In the present paper, we report the chemical analysis of two carbon stars belonging to a more (on average) metal-poor environment: the Carina dwarf Spheroidal galaxy. The aim of these works is to observationally test the predicted critical dependence on the stellar metallicity (mass) of the *s*-process nucleosynthesis in AGB stars (and of their carbon enrichment). Also, by studying the *intrinsic index* abundance ratio [*hs*/*ls*] in AGB stars of different metallicity, it is possible to better constraint the total neutron flux in the *s*-process: the ^{13}C efficiency.

The paper is structured as follows: Sect. 2 presents the selected stars and the observations. The chemical analysis is described in Sect. 3. In Sect. 4 we discuss the abundance pattern found in the framework of the *s*-process nucleosynthesis models in AGB stars and, finally, we draw some conclusions in Sect. 5.

[1] Here we use the standard notation for the chemical abundance ratio of any element *X*, $[X/H] = \log (X/H)_{\star} - \log(X/H)_{\odot}$, where log (H) ≡ 12 is the abundance of hydrogen by number. In this scale the abundance of any element is noted as $\epsilon(X)$.

2. Carbon-rich stars in Carina and observations

Following the chemical study of carbon stars in the SMC and the Sagittarius dSph (Paper I), the Carina dSph galaxy was found to be another interesting target in terms of carbon star population and the brightness of such stars. Carina is located at a distance of about 95 kpc (Mighell 2006) and suffers an interstellar extinction $A_B = 0.271^{mag}$ (NASA/IPAC database, Schlegel et al. 1998). As mentioned above, the metallicity of its stellar component ranges from 0.0 to −3.0 with a mean of [Fe/H] ≈ −1.8 (Koch et al. 2006; see also Helmi et al. 2006).

Few carbon stars are still known in Carina (only nine) and we selected for this work two of its brightest members (ALW-C6 & ALW-C7) from Azzopardi et al. (1986, we adopt their naming convention). Before the present study, these two stars were already spectroscopically confirmed to be carbon-rich by Linden-Bell et al. (1983). The photometric properties of ALW-C6 and ALW-C7 are reported in Table 1. The *JHK*-magnitudes are from the Two Micron All Sky Survey (Skrutskie et al. 1997). We also report in this table our estimates of their bolometric luminosity using the calibration of Alksnis et al. (1998), assuming that this can be safely applied to metal-poor carbon stars. The bolometric magnitudes derived are compatible with those expected for low mass TP-AGB stars undergoing TDU (Straniero et al. 2003), even if large uncertainties in the estimated M_{bol} values are considered.

The selected carbon stars were observed in service mode with the UVES spectrograph attached to the second VLT unit. These spectra were collected in December 2004 with the same configuration as in Paper I (standard settings *Dichroic*2, *CD*#2 centred at 4370 Å and *CD*#4 centred at 8600 Å, 1″ slit width corresponding to a resolving power of about 40 000). The air masses of the observations were always smaller than 1.2 and the mean seeing was ∼0.8″ and ∼0.6″ for ALW-C6 and ALW-C7, respectively (see also Table 1). The available spectral domains are from ∼4200 to ∼5000 Å and from ∼6700 to ∼9000 Å. However, we point out that below ∼4750 Å, the spectra quality was found to be rather poor ($S/N \sim 20-30$) due to the faintness of these stars in the blue. The spectra were reduced with the UVES Data Reduction Standard pipeline. Then, for each star and spectral range, they were averaged and corrected to the local standard of rest. By measuring the wavelengths of several strong atomic features, we estimated a radial velocity of 224.4 and 224.7 ± 0.5 km s^{-1} for ALW-C6 and ALW-C7, respectively (our velocity resolution is about 40 km s^{-1}). These values perfectly agree with the systemic velocity of Carina dSph quoted by Mateo (1998) and Majewski et al. (2005). Finally, all the spectra were normalised to the local continuum by fitting a polynomial connecting the higher flux points in the spectral regions studied. We note that, in the blue part of its spectrum, the uncertainty in the continuum location might reach ∼5% in ALW-C6 because of the rather low S/N ratio achieved for this star here (see Paper I for more details on the normalisation procedure). We also point out that the spectrum of ALW-C7 shows a weak H_{β} line in emission.

3. The Carina carbon stars and their chemical properties

Chemical analysis of the Carina carbon stars was performed following the procedure described in Paper I. Briefly, LTE spectral synthesis of specific spectral regions in the optical were performed in order to derive the chemical abundances of the CNO elements, the carbon isotopic ratio, Li, *s*-elements and the mean metallicity [M/H], this latter being obtained from the

Table 1. Carbon stars observation log and photometric properties.

Star	Instrument	Date Obs.	Exp. time (min)	V	J	H	K	M_{bol}
Carina ALW-C6	UVES	2004-12-2/3/4	120	16.4	13.7	12.8	12.3	–4.7
Carina ALW-C7	UVES	2004-12-04	120	16.5	14.2	13.2	12.7	–4.3

Table 2. Main atmospheric parameters of the Carina carbon stars. See text for details.

Star	$T_{\rm eff}$(K)	[M/H]	C/O	ϵ(C)−ϵ(O)	^{12}C/^{13}C
ALW-C6	3400	−2.00	5–8	7.8	≥125
ALW-C7	3200	−2.00	4–6	7.2	≥250

mean value derived from lines of Ca, Ti, V, Mn, Fe and Ni. According to Shetrone et al. (2003), there is no evidence of any α-enhancement pattern in Carina, although the giant stars analysed by these authors exhibit a large dispersion in the α-element content, which they interpreted as an indication of a bursting star formation history. Therefore, the Ca and Ti abundances derived were also used as metallicity indicators (however, see Sect. 4 for ALW-C7). Table 2 shows the metallicity of the model atmospheres used. The adopted solar abundances for C, N and O in the models are 8.41, 7.80 and 8.67 (Asplund et al. 2005a).

We used the same atomic and molecular line lists and model atmospheres for cool carbon-rich stars (assuming 2 $M_{\odot}$) as in Paper I (see this paper for details). The atomic line lists in the spectral ranges of interest were once again extended using the recent atomic line data base DREAM[2], and corrected by comparison with a high resolution spectrum of Arcturus. However, comparison between theoretical and the observed spectra of ALW-C6 and ALW-C7 revealed that our atomic and molecular lists (especially the latter) are still far from being complete (see figures below).

A first guess of the effective temperatures was estimated from the calibrations of the $(H-K)_{\rm o}$ and $(J-K)_{\rm o}$ colour indexes by Bergeat et al. (2001). We avoided the $(V-K)_{\rm o}$ vs. $T_{\rm eff}$ calibration because the V-magnitudes of these probable variable stars were collected at a very different epoch to the other infrared indexes. The final adopted values (Table 2) were obtained through an iterative process by comparing the observed optical spectra with theoretical ones. The first guesses obtained from the calibrations by Bergeat et al. (2001) were cooler than those finally adopted in Table 2. The iterative process also included the C/O ratio (or the abundance difference ϵ(C)−ϵ(O), hereafter C−O) and the metallicity adopted in the model atmosphere. These are the main atmosphere parameters that determine the global shape of the synthetic spectrum (gravity has only a minor effect). Note that AGB stars are typically variable and since the UVES spectra and the infrared photometry were not collected at the same epoch, the specific $T_{\rm eff}$ value that provides the best fit to the optical spectra may differ from the photometric estimates. The only meaningful way of describing the observations of variable stars would be to ascribe one pulsating model atmosphere to the star, and explain the different observations as different phases of this model. This is, however, beyond the scope of this paper (see Gautschy-Loidl et al. 2004; Lederer et al. 2006, for recent advances in pulsational model atmospheres). As in Paper I, we estimate that the $T_{\rm eff}$ uncertainty is around ±250 K.

The gravity was set at $\log g = 0.0$ for the two stars. This value agrees with that estimated using the classical formulae relating gravity to effective temperature and luminosity, adopting a stellar mass of 2 $M_{\odot}$. The error in gravity, due mainly to the uncertainty in the mass and somewhat to luminosity is, however, as large as ±0.5 dex although this uncertainty has minor effects on the chemical abundances derived. The microturbulence parameter initially adopted was $\xi = 2.2$ km s^{-1} (Lambert et al. 1986), although beyond 6700 Å, larger values were used (3−4 km s^{-1}) to fit the strong (probably saturated) molecular CN and C_2 lines present in this spectral region. The uncertainty in this parameter, independent of the spectral region studied, is of the order of ±0.5 km s^{-1}. Synthetic spectra were broadened with a Gaussian function to match the instrumental profile and with a macroturbulence velocity ranging from 4 to 7 km s^{-1}.

To perform the chemical analysis of the UVES spectra we followed the same procedure as in Paper I. The large carbon enhancement of these stars (see Table 2) complicated their chemical analysis. The spectral region between 4750−4950 Å, typically used to derive metallic abundances in Paper I and in other AGB carbon stars with higher metallicity, appears very crowded by molecular lines (mainly CH and C_2) in ALW-C6 and ALW-C7. These molecular features dominate the global absorption in this spectral region, while in galactic ([Fe/H] ∼ 0), less carbon-enhanced (C/O ∼ 1−2) AGB carbon stars, atomic lines are the main contributors (e.g. Abia et al. 2002). This is probably a metallicity effect that gives stronger C_2 and CH bands at lower metallicity for a given C/O ratio (or C−O). This is partly due to less carbon being locked up in CN, CS etc., thus favouring the formation of C_2 and CH. This can be seen in Fig. 1 that shows a theoretical fit in this region for the star ALW-C7. It is particularly interesting to compare this figure with Fig. 2 of Paper I: ALW-C7 shows very broad spectral features, many of them not reproduced by our synthetic spectrum at all. We believe that most of these features are molecular lines missing from our line list. Note also that many spectral features due to *s*-elements are present; some are very strong, revealing evidence of a large *s*-elements enhancement. Unfortunately, many of these strong spectral features are blends of several *s*-element lines with uncertain oscillator strengths that preclude their use as abundance indicators. A similar situation occurs with metallic lines: only a few of them were used because of their weakness due to the metal deficiency of the Carina stars[3]. Figure 2 shows a theoretical fit to ALW-C6 in another spectral region.

Similarly to what was found in Paper I and in other studies of carbon stars (e.g. Uttenthaler et al. 2006), the derived C/O ratio slightly decreases with the wavelength of the analysed spectral region. This is because below ∼4900 Å, lines seem to be more pronounced in the theoretical spectra than in the observed one. However, we found that the difference between the corresponding C/O ratios derived never exceeds a factor of ∼1.5. The reason for this discrepancy is still unknown. Another source of uncertainty in the derivation of the C/O ratio is the fact that synthetic spectra computed with O abundances differing by a large factor cannot be distinguished, which allows a range of C/O ratios (or the difference C−O) to give good fits to the observed spectra (see

[2] http://w3.umh.ac.be/astro/dream.shtml

[3] Note the small number of metallic lines detected in Fig. 1 as compared to Fig. 2 in Paper I.

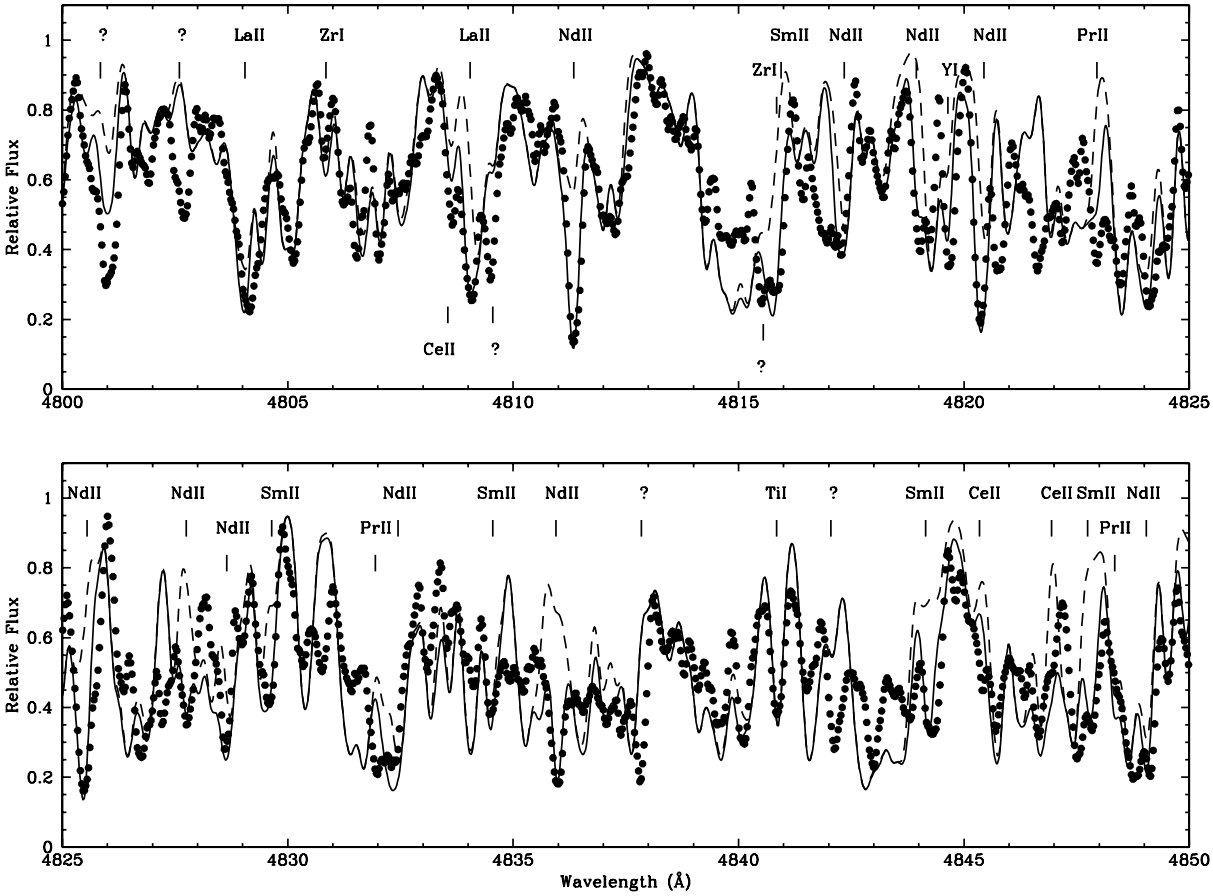

Fig. 1. Synthetic fit to the spectrum of ALW-C7 in the region around λ4825 Å. Black dots represent the observed spectrum. Lines are synthetic spectra: only molecules and metals (dashed line), and including *s*-elements (continuous line) using the mean values for the abundances shown in Table 4. Some spectral (probably molecular) features, not reproduced by the synthetic spectrum, as well as some atomic lines, are marked.

the detailed explanation in Paper I). Unfortunately, we cannot derive the absolute O abundance independently of the available spectra. Therefore, we take the O abundance as a free parameter scaled with the metallicity. Due to this, in Table 2 we give a range of values for the C/O ratio and the average abundance difference ϵ(C)−ϵ(O). This ambiguity in the C/O ratio, however, does not affect the ^{12}C/^{13}C ratio derived from ^{12}CN and ^{13}CN features in the ∼8000 Å range. The best fits to the ^{13}CN lines in this region give 125 and 250 for the carbon isotopic ratio in our stars (see Table 2). Nevertheless, since theoretical spectra computed with an isotopic ratio a factor ∼2 lower (higher) do not differ significantly, we consider these ratios only as lower limits. Furthermore, theoretical fits of the ^{13}C^{12}C band (probably saturated) at ∼4730 Å in both stars lead to isotopic ratios slightly larger than those quoted in Table 2.

A full discussion about the sources of error in the absolute abundances and element ratios due to uncertainties in the atmosphere parameters, continuum location and random errors when a given element is represented by a few lines, as it is our case, can be found in Abia et al. (2001, 2002) and will not be repeated here. These errors range from ±0.2 dex for Ba to ±0.5 dex for Ce and Li. We estimate a typical uncertainty in the mean metallicity ([M/H]) of ±0.30 dex. Errors for the elemental ratios with respect to the metallicity ([*X*/M]) range between 0.3−0.4 dex, since some of the uncertainties cancel out when deriving this ratio. For the same reason, the error in the abundance ratio between elements ([*X*/*Y*]) is somewhat lower, ±0.3 dex. These numbers do not include possible systematic errors such as N-LTE effects or an uncertainty larger than 5% in the continuum location, as might be the case in the spectrum of ALW-C6.

4. Results and discussion

Table 3 shows the metal abundances derived in ALW-C6 and ALW-C7. Other than the species shown in this table, both stars present a significant number of absorptions due in part to interesting species like Cr, Ru, Gd and W. Many spectral blends are reproduced better with synthetic spectra assuming some *r*-element enhancement. This is a very relevant point which merits confirmation using spectra with much higher spectral resolution and a more complete (accurate) molecular line list. However, due to the severe blending and uncertain oscillator strengths, we discarded these features as abundance indicators in the present study.

We now present the main chemical properties of the analysed stars:

These stars are not Li-rich; their derived Li abundances are similar to the average value derived in galactic AGB carbon stars (Denn et al. 1991; Abia et al. 1993). ALW-C6 and ALW-C7 are the most metal-poor C-rich stars ever chemically analysed in any external galaxy. The derived metallicities (Table 4) agree with the average value previously obtained in the stellar populations of Carina dSph (see Sect. 1).

On the other hand, we found some enrichment of Ti in ALW-C6 ([Ti/M] = +0.3) with respect to the other metallicity indicators and, in contrast, some deficiency in ALW-C7

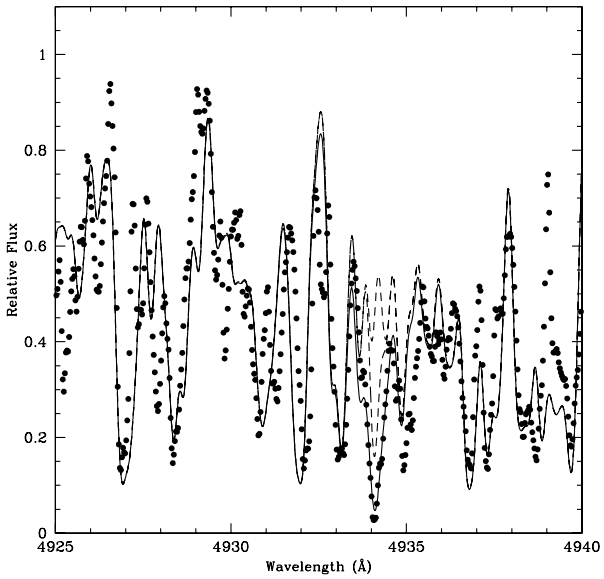

Fig. 2. Synthetic fit to the spectrum of ALW-C6 in the region of the Ba II line at λ4934 Å. Black dots represent the observed spectrum. Lines are synthetic spectra for different [Ba/M] ratios: no Ba and +0.0 (dashed lines), +2.0 (best fit, continuous line).

Table 3. Summary of the abundances derived in the programme stars. *N*, indicates the number of lines utilised for a specific element when more than one line is used (we then give the mean abundance together with its dispersion). [el/M] is the abundance ratio with respect to the mean metallicity derived [M/H] (see text) and is only quoted for elements with $A \geq 30$. The [el/M] ratios are calculated with respect to the solar photospheric abundances according to Asplund et al. (2005b).

	ALW-C6			ALW-C7		
Element	*N*	$\epsilon(\times)$	[el/M]	*N*	$\epsilon(\times)$	[el/M]
Li		0.00			−0.50	
Ca		4.60			4.30	
Ti	2	3.50 ± 0.10		2	2.60 ± 0.15	
V	2	2.30 ± 0.20			2.10	
Mn	2	3.70 ± 0.10		2	3.10 ± 0.20	
Fe		–			5.50	
Ni	2	4.40 ± 0.02		2	4.20 ± 0.05	
Zn		3.00	+0.10		–	
Rb		–			<1.00	<+0.3
Sr		–			<1.90	<+0.9
Y	2	1.90 ± 0.00	+1.4	3	0.80 ± 0.05	+0.5
Zr	3	1.90 ± 0.10	+1.0	3	0.90 ± 0.10	+0.2
Ba		2.50	+2.0		2.10	+1.8
La	2	0.90 ± 0.00	+1.5	3	0.90 ± 0.15	+1.7
Ce		<1.80	<+1.9	2	1.80 ± 0.05	+2.1
Nd	4	1.75 ± 0.25	+2.0	5	1.70 ± 0.10	+2.1
Sm	3	1.00 ± 0.03	+1.7	4	1.10 ± 0.00	+2.0
Hf		<1.20	<+2.0		<0.60	<+1.6

([Ti/M] = −0.4). This apparent dispersion in the Ti abundance among the stars of Carina is also found by Shetrone et al. (2003) in several RGB stars. These authors found a [Ti/Fe] ratio below solar in their star named Car 3. Car 3 also shows undersolar [Mg, Si, Ca/Fe] ratios. Shetrone et al. interpreted this α-element deficiency in terms of the star formation history in Carina dSph. In our case, and due to the small number of Ti lines used, and to the large abundance errors, we cannot definitely conclude that ALW-C6 or ALW-C7 is α-enhanced or depleted, respectively. Note for instance that the Ca abundances derived in both

Table 4. Metallicity and *s*-process indexes derived in Carina C-stars. Abundance upper limits in Table 4 were disregarded in computing these abundance indexes.

Star	[M/H]	[*s*/M]	[*ls*/M]	[*hs*/M]	[*hs*/*ls*]
ALW-C6	−1.7	+1.60	+1.20	+1.80	+0.60
ALW-C7	−1.9	+1.50	+0.35	+1.90	+1.55

stars are compatible with [Ca/M] ∼ 0.0. Nevertheless, in the case of ALW-C7, the possible Ti depletion might have another interesting explanation (see below). Our analysis also indicates that ALW-C7 is moderately deficient in Mn, [Mn/M] = −0.3. Shetrone et al. (2003) found a similar Mn deficiency in all their Carina RGB stars. In galactic clusters and/or field stars with similar metallicity to ALW-C7, Mn seems to be deficient relative to Fe by a similar amount (e.g. Sobeck et al. 2006). On the other hand, the [Zn/M] ratio derived in ALW-C6 is consistent with the figure observed in galactic metal-poor stars (see Mishenina et al. 2000; Saito et al. 2006) with the same metal deficiency.

Another relevant issue is the extrinsic or intrinsic nature of the carbon stars analysed. The available photometric indexes and the derived luminosities and stellar parameters (see Tables 1 and 2) suggest that these stars are on the AGB phase. In fact, normal (spectral type N) carbon rich AGB stars are commonly placed in the colour diagram $(J - H)$ vs. $(H - K)$ in the region $(H - K) > 0.4$ and $(J - H) > 0.8$ (Knapp et al. 2001). The infrared colours of ALW-C6 and ALW-C7 fulfil this requirement. Unfortunately, the detection of Tc lines or/and the study of the [Nb/Zr] ratio in our stars, two powerful nucleosynthesis indicators of an intrinsic nature, were not possible. The *s*-element Nb is the product of the radiogenic decay of ^{93}Zr ($\tau_{1/2}$ = 1.5 Myr), which is strongly fed by the *s*-process. For intrinsic AGB stars a [Zr/Nb] ≈ 1 is expected, whereas for an extrinsic AGB, [Zr/Nb] ≈ 0.0 (e.g. Ivans et al. 2005). On the other hand, to our knowledge, there are no studies on the possible luminosity variations of these stars, a common characteristic of the stars on the AGB. Therefore, a final answer cannot be given regarding the extrinsic or intrinsic nature of these two carbon stars. The evidence of a young stellar population in Carina (∼2 Gyr, see Sect. 1) is compatible with the presence there of stars currently in the AGB phase.

Independently of their extrinsic or intrinsic nature, the *s*-element enhancements found in both stars can be directly compared with theoretical *s*-process nucleosynthesis calculations (see Fig. 3). Indeed, in the extrinsic case, observations can be interpreted from models just introducing a proper dilution factor to simulate the mixing effect of the AGB winds with the convective envelope of the observed star. This dilution factor would affect by the same amount all the element abundances. In consequence, the abundance ratios between two elements will not be affected by this dilution. The average *s*-element enhancement in ALW-C6 and ALW-C7 ([*s*/M] in Table 4) is similar to that found in galactic metal-poor ([Fe/H] ≤ −1.5) carbon stars (e.g. Aoki et al. 2002; Lucatello et al. 2003; Barbuy et al. 2005; or references in Beers & Christlieb 2005). Note that the overwhelming majority of these galactic stars are binary (extrinsic, Lucatello et al. 2005), where the more massive companion, while on the AGB, transferred part of its C-rich and *s*-rich material to the star now observed. At the metallicity of our stars, a greater enrichment of the heavy-*s* elements compared to the light-*s* elements is expected. This is because the number of neutrons captured per seed nucleus (^{56}Fe) increases with decreasing metallicity and the *s*-process overcomes the ls peak favouring the

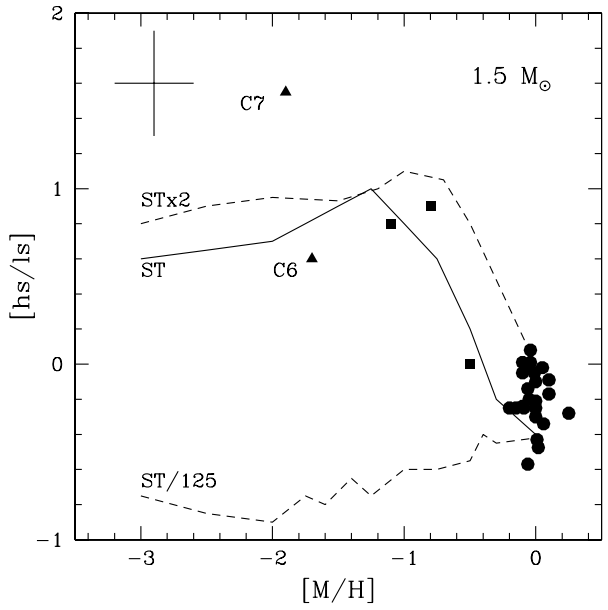

Fig. 3. The derived $[hs/ls]$ ratios vs. [M/H] in ALW-C6 and ALW-C7 (triangles) compared with theoretical *s*-process nucleosynthesis predictions in a 1.5 $M_{\odot}$ TP-AGB star for different choices of the ^{13}C-pocket. Squares are the C-stars belonging to the SMC and the Sagittarius dSph studied in Paper I. Solid circles are the galactic AGB C-stars from Abia et al. (2002). See text for details.

formation of *s*-elements of the second peak (Ba, La, Ce etc.). This is what we observe in the carbon stars of Carina (see Tables 3 and 4), $[hs/ls] > 0$. Moreover, at the metallicity of our stars, it is predicted that the second *s*-peak also will be overcome by the *s*-process fluency, feeding the termination point of the *s*-path at ^{208}Pb. Very high [Pb/Fe] ratios are therefore expected (e.g. Gallino et al. 2006; Cristallo 2006). This is what is observed in very metal poor *s*-element enriched galactic stars (all extrinsic) (e.g. Van Eck et al. 2003; Ivans et al. 2005, and references therein). Unfortunately, the available Pb lines at ~4000 Å cannot be detected in C-rich AGB stars since they are too faint.

The derived $[ls/M]$, $[hs/M]$ and $[hs/ls]$ ratios in our stars might be reproduced theoretically (within the uncertainties) with a proper choice of the ^{13}C pocket and initial stellar mass. In fact, the different choices of these parameters allow a large spread of these *s*-process indexes at any metallicity, covering more than two orders of magnitude (this spread is smaller for the $[hs/ls]$ ratio). The observations in galactic AGB (extrinsic and intrinsic) and post-AGB stars seems to confirm this spread. In our case, the *s*-element abundance ratios for ALW-C6 in Table 4 can be accounted for (considering the uncertainties) with a $Z \sim 10^{-4}$ AGB star model with a mass lower than 2.0 $M_{\odot}$ and a ^{13}C pocket choice within a factor of 3 above and below around the ST case (see Sect. 1 and Gallino et al. 2006). In the case of ALW-C7, the stellar mass model should be lower than 1.5 $M_{\odot}$, but although the derived $[ls/M]$ and $[hs/M]$ indexes can be reproduced within similar choices for the ^{13}C pocket, the observed $[hs/ls]$ index is too high compared to the theoretical predictions. This can be clearly seen in Fig. 3, where the continuous line corresponds to the prediction for the ST (standard) ^{13}C-pocket choice and dashed lines limit the area allowed by theoretical models for the different pocket choices (in the figure from ST/125 to ST × 2; see Gallino et al. 2006). This is due to the low light-*s* enhancement found in this star relative to the heavy-*s* enhancement, in particular the Zr abundance (see Table 5). If we exclude a severe error in the abundance analysis, this figure has no easy explanation. According to the standard theoretical calculations of the main component of the *s*-process in low mass AGB stars, the enhancement should be similar for Y and Zr, i.e. [Zr/Fe] ~ [Y/Fe] (actually, slightly higher for Zr), whatever the choice of the stellar mass model, ^{13}C-pocket etc. However, we have found that the [Y/M] ratio significantly exceeds the [Zr/M] one in both stars[4] (see Table 3). The differences are larger than the expected error in the [X/M] ratios (~0.3 dex), in particular for ALW-C7. We think that this difference cannot be ascribed to incorrect gf-values of the Zr and Y lines, as we have used the same lines as in our previous analyses of carbon stars (Abia et al. 2002; Paper I), where a good agreement was found between Zr and Y enhancements. Note also that the dispersion around the mean abundances for both elements (see Table 3) is relatively small. Thus, except assuming an incorrect derivation of the model atmosphere parameters, or molecular blends, this difference may be real.

It is interesting to note that Zr lines are weaker in the spectra of ALW-C6 and ALW-C7 compared to the same Zr lines in the stars analysed in Paper I. We checked that the difference in intensity cannot only be explained by a difference in the metallicity of the stars[5]. The stars here and in Paper I have similar $T_{\rm eff}$ and gravity values. A possible explanation for this difference would be to admit some Zr depletion into dust grains formed in the circumstellar envelope around these stars (in ALW-C7 in particular). In C-rich circumstellar envelopes (C/O > 1), a refractory element such as Zr condenses into ZrC for any pressure, at a temperature about 500 K higher than Y does in YC_2 (see e.g. Lodders & Fegley 1995; Lodders & Amari 2005). According to these authors, the temperature condensation sequence for trace elements (such as Zr) is TaC, WC, NbC, ZrC, HfC, TiC and then, YC_2 at much lower temperature than the former molecules. Other refractory *s*-element such as Ba, La and Ce condense at much lower temperatures. Therefore, an important depletion of these heavy-*s* elements in the gas phase is not expected. Theoretical calculations show that the condensation temperature increases with the C/O ratio and with increasing element abundances: i.e. ZrC will form more easily in the circumstellar envelope of a carbon-rich AGB star, the larger the C/O ratio and the greater the Zr enhancement. Ti has a condensation temperature only ~150 K lower than Zr independent of the actual C/O ratio and partial pressure. Thus, the moderate Ti deficiency found in ALW-C7 (see Table 3 and the discussion above) might be another indication of some photospheric depletion in this star. This might explain why some depletion is observed at least in ALW-C7 (with a large C/O ratio) and not in less carbon enhanced stars such as those of Paper I and/or in their galactic counterparts (Abia et al. 2002). This result is preliminary and requires further and careful studies using much higher spectral resolution. In particular, a typical depletion pattern showing lower abundances for elements with higher condensation temperature should be found. Also, quantitative calculations of the expected Zr depletion factor and how it may vary with the C/O ratio and average metallicity are required before arriving at any conclusions.

[4] In many C-rich metal-poor galactic stars the opposite is found, i.e. [Y/Fe] ≪ [Zr/Fe] (see Bisterzo et al. 2006, and references therein). Nevertheless, this difference seems to be a spectroscopic problem rather than a nucleosynthetic one.

[5] Compare Zr lines in Figs. 1 (ALW-C7) and 2 (IGI95-C1) in this work and Paper I, respectively.

Finally, to our knowledge, the C/O ratios derived in ALW-C6 and ALW-C7 are the largest values ever found in a C-rich AGB star assuming that both stars are intrinsic. Domínguez et al. (2004) discovered another (probably) AGB star (D461), belonging to the Draco dSph galaxy, with some carbon enhancement, C/O ∼ 3. D461 is also a very metal-poor star ([Fe/H] ∼ −2.0). C/O ratios larger than unity are expected in the envelopes of low mass AGB stars as a consequence of the mixing of ^{12}C from the He inter-shell trhough the TDU. Due to the lower O content in the envelopes of metal-poor stars and because the efficiency of TDUs increases as metallicity drops, the lower the metallicity of the star, the large C/O ratio that is expected in the envelope. The C/O ratios found in our stars agree with this prediction. Solar metallicity galactic AGB carbon stars typically show smaller ratios, C/O ∼ 1−2 (Lambert et al. 1986; Abia et al. 2002). Observational evidence that AGB stars in metal deficient environments show greater carbon enhancements has also been found in the Magellanic Clouds (Matsuura et al. 2002). Nevertheless, the actual carbon enhancements are difficult to reconcile with low mass metal-poor AGB models. The problem is that C/O ratios as high as those derived in ALW-C6 and ALW-C7 are easily obtained in theoretical models after a few TDU episodes (actually one of two TDUs). For such a low number of TDU episodes, the enrichment of the envelope in *s*-elements is however moderate, [*s*/Fe] < +0.5. In fact, a significant number of TDU episodes are needed to obtain the *s*-element abundance ratios observed in our stars. For instance, in the 2 $M_{\odot}$, $Z = 10^{-4}$ AGB model of Cristallo (2006), which may resemble the stars analysed here, more than 6 TDU mixing events are required. However, after 6 TDU episodes, the C/O ratio in the envelope in such model is ∼40 and the ^{12}C/^{13}C > 500, values that largely exceed those derived in ALW-C6 and ALW-C7. In brief, the *s*-element and ^{12}C enhancement observed in the Carina stars are difficult to reconcile simultaneously by current low mass metal-poor AGB models. Note, nevertheless, that model predictions are very much dependent on the opacity treatment in the envelope, on the parametrisation of the mass loss rate history, the mixing details and its efficiency, etc. (Chieffi et al. 2001; Cristallo et al. 2007). These factors have a critical influence on the occurrence of the TDU episodes, their efficiency as well as on the duration of the AGB phase. As a consequence, they determine the level of carbon and *s*-element enrichment in the envelope at a given TP and TDU episod. This means that eventually it should be possible to reconcile observations and model predictions with a proper choice of these two uncertain parameters. A detailed discussion of this topic will be presented elsewhere (Domínguez et al. 2008, in preparation). Note, on the other hand, that many of the very metal-poor dwarfs and giants in the halo and field of the galaxy show large carbon and *s*-element enhancements ([*s*, C/Fe] > 1; see e.g. Aoki et al. 2007). The majority of these stars are extrinsic, i.e. they have accreted material from a companion (now a white dwarf) when it was on the AGB phase. In those stars where the oxygen abundance has been determined, the corresponding C/O ratio range from near 1 to almost 100 (e.g. Sivarini et al. 2006), indeed suggesting that C/O ratios much larger than those derived in our stars eventually can be reached in the envelopes of AGB stars[6].

[6] Note that it is difficult to estimate the original C/O ratio in the transferred material from these observations due to the unknown dilution factor with the envelope of the secondary and possible O production during the AGB phase (Herwig 2004).

5. Summary

In this paper we have presented a detailed chemical analysis of two carbon stars belonging to the Carina dSph using high resolution optical spectra. Their observational properties and derived chemical abundances suggest that both stars are currently in the AGB phase undergoing TDU and TP episodes. Despite to the large uncertainties in the analysis, their derived metallicity is compatible with the average metallicity of the stellar main component of Carina derived by previous studies. In fact, their low metallicity ([Fe/H] ∼ −2.0) does not ease their abundance analysis since their spectra are completely dominated by molecular (C-bearing) absorptions. Nevertheless, the analysis of molecular bands reveals that ALW-C6 and ALW-C7 have large carbon enhancements (C/O > 4), which makes these stars the most C-rich AGB stars ever observed. Both stars also show large *s*-element enhancements, which are in agreement with theoretical *s*-process nucleosynthesis predictions in low-mass metal-poor AGB models on the basis that the ^{13}C$(\alpha, n)^{16}$O reaction is the main source of neutrons. However, there are still difficulties to simultaneously explain the large ^{12}C/^{13}C ratio, the carbon abundance and the *s*-process enhancements found in the framework of the current theoretical TP-AGB models.

Acknowledgements. This publication makes use of data products from the Two Micron All Sky Survey, which is a joint project of the University of Massachusetts and the Infrared Processing and Analysis Center/California Institute of Technology, funded by the National Aeronautics and Space Administration and the National Science Foundation. We would like to thank B. Plez for his help with the molecular line lists. Part of this work was supported by the Spanish grant AYA2005-08013-C03-03 from the MEC. P. de Laverny acknowledges the financial support of Programme National de Physique Stellaire (PNPS) of CNRS/INSU, France.

References

Abia, C., Boffin, H. M. J., Isern, J., & Rebolo, R. 1993, A&A, 272, 455
Abia, C., Busso, M., Gallino, R., et al. 2001, ApJ, 559, 1117
Abia, C., Domínguez, I., Gallino, R., et al. 2002, ApJ, 578, 817
Alksnis, A., Balnauss, A., Dzervitis, V., & Eglitis, I. 1998, A&A, 338, 209
Aoki, W., Ryan, S. G., Norris, J. E., et al. 2002, ApJ, 580, 1149
Aoki, W., Beers, T. C., Christlieb, N., et al. 2007, ApJ, 655, 492
Asplund, M., Grevesse, N., Sauval, A. J., et al. 2005a, A&A, 431, 693
Asplund, M., Grevesse, N., & Sauval, A. J. 2005b, in Cosmic Abundance as Records of Stellar Evolution and Nucleosynthesis, ed. T. G. Barnes, & F. N. Bash, ASP Conf. Ser., 336
Azzopardi, M., Lequeux, J., & Westerlund, B. E. 1986, A&A, 161, 232
Barbuy, B., Spite, M., Spite, F., et al. 2005, A&A, 429, 1031
Beers, T. C., & Christlieb, N. 2005, ARA&A, 43, 531
Bergeat, J., Knapik, A., & Rutily, B. 2001, A&A, 369, 178
Bisterzo, S., Gallino, R., Straniero, O., et al. 2006, in Origin of Matter and Evolution of Galaxies, AIP Conf. Ser., 847, 368
Busso, M., Gallino, R., & Wasserburg, G. 1999, ARA&A, 37, 329
Busso, M., Lambert, D. L., Gallino, R., Travaglio, C., & Smith, V. V. 2001, ApJ, 557, 802
Busso, M., Calandra, A., & Nucci, M. C. 2006, MemSAI, 77, 798
Cannon, R. D., Niss, B., & Nœrgaard, H. U. 1981, MNRAS, 196, 1
Chieffi, A., Domínguez, I., Limongi, M., & Straniero, O. 2001, ApJ, 554, 1159
Cristallo, S. 2006, PASP, 118, 1360
Crsitallo, S., Straniero, O., Lederer, M. T., et al. 2007, ApJ, 667, 489
de Laverny, P., Abia, C., Domínguez, I., et al. 2006, A&A, 446, 1107, Paper I
Denn, G. R., Luck, R. E., & Lambert, D. L. 1991, ApJ, 377, 657
Domínguez, I., Abia, C., Straniero, O., Cristallo, S., & Pavlenko, Ya. 2004, A&A, 422, 1045
Gallino, R., Arlandini, C., Busso, M., et al. 1998, ApJ, 497, 388
Gallino, R., Bisterzo, S., Straniero, O., Ivans, I. I., & Kaeppeler, F. 2006, MemSAI, 77, 786
Gautschy-Loidl, R., Höfner, S., Jørgenssen, U. G., & Hron, J. 2004, A&A, 422, 289
Goriely, S., & Siess, L. 2001, A&A, 378, L25

Goriely, S., & Siess, L. 2004, A&A, 421, L25
Helmi, A., Irwin, M. J., Tolstoy, E., et al. 2006, ApJ, 651, L121
Herwig, F. 2004, ApJS, 155, 651
Herwig, F. 2005, ARA&A, 43, 435
Ivans, I. I., Sneden, C., Gallino, R., et al. 2005, ApJ, 627, 145
Knapp, G. R., Pourbaix, D., & Jorissen, A. 2001, A&A, 371, 222
Koch, A., Grebel, E. K., Wyse, R. F., et al. 2006, AJ, 131, 895
Lambert, D. L., Gustafsson, B., Eriksson, K., & Hinkle, K. H. 1986, ApJS, 62, 373
Lanfranchi, G. A., Matteucci, F., & Cescutti, G. 2006, A&A, 453, 67
Lederer, M., Lebzelter, T., Aringer, B., et al. 2006, MemSAI, 77, 1008
Lynden-Bell, D., Cannon, R. D., & Godwin, P. J. 1983, MNRAS, 204, 87
Lodders, K., & Fegley, B. 1995, Meteoritics, 30, 661
Lodders, K., & Amari, S. 2005, Chemie der Erde, 65, 93
Lucatello, S., Gratton, R., Cohen, J. G., et al. 2003, AJ, 125, 875
Lucatello, S., Tsangarides, S., Beers, T. C., et al. 2005, ApJ, 625, 825
Majewski, S. R., Frinchaboy, P. M., Kunkel, W. E., et al. 2005, AJ, 130, 2677
Mateo, M. 1998, ARA&A, 36, 435
Matsuura, M., Zijlstra, A. A., van Loon, J. Th., et al. 2002, ApJ, 580, L133
Mighell, K. J. 1997, AJ, 114, 1458
Mishenina, T. V., Koutyukh, V. V., Soubiran, C., Travaglio, C., & Busso, M. 2002, A&A, 396, 189
Monelli, M., Pulone, L., Corsi, C. E., et al. 2003, AJ, 126, 218
Mould, J. R., Cannon, R. D., Forgel, J. A., & Aaronson, M. 1982, ApJ, 254, 500
Rizzi, L., Held, E. V., Bertelli, G., & Saviane, I. 2003, ApJ, 598, L85
Saito, Y.-J., Takada-Hidai, M., Takeda, Y., Honda, S., & Katsumata, M. 2006, in Origin of Matter and Evolution of Galaxies, AIP Conf. Ser., 847, 464
Schlegel, D. J., Finkbeiner, D. P., & Davis, M. 1998, ApJ, 500, 525
Shetrone, M., Venn, K. A., Tolstoy, E., et al. 2003, AJ, 125, 684
Siess, L., Goriely, S., & Langer, N. 2004, A&A, 415, 1089
Sivarini, T., Beers, T. C., Bonifacio, P., et al. 2006, A&A, 459, 125
Skrutskie, M. F., Schneider, S. E., Stiening, R., et al. 1997, in The Impact of Large Near-IR Sky Surveys, ed. F. Garzon et al. (Dordrecht: Kluwer Academic), 25
Smecker-Hane, T. A., Stetson, P. B., Hesser, J. E., Lehvert, M. D., & VanderBerg, A. 1996, in From stars ti Galaxies: The impact of stellar physics on galaxy evolution, ed. C. Leitherer, V. Fritze-von Aliensleben, & J. Huchra, AIP Conf. Ser., 328
Sobeck, J. S., Ivans, I. I., Simmerer, J. A., et al. 2006, AJ, 131, 2949
Straniero, O., Gallino, R., Busso, M., et al. 1995, ApJ, 440, L85
Straniero, O., Domínguez, I., Cristallo, S., & Gallino, R. 2003, PASA, 20, 389
Uttenthaler, S., Hron, J., Lebzelter, T., et al. 2006, MemSAI, 77, 961
Van Eck, S., Goriely, S., Jorissen, A., & Plez, B. 2003, A&A, 404, 291
van Winckel, H. 2003, ARA&A, 41, 391